

## Bent bonds, the antiperiplanar hypothesis and the theory of resonance. A simple model to understand reactivity in organic chemistry

Ghislain Deslongchamps<sup>\*a</sup> and Pierre Deslongchamps<sup>\*b,c</sup>

Received 13th March 2011, Accepted 12th May 2011

DOI: 10.1039/c1ob05393k

By taking into consideration bent bonds ( $\tau$ -bonds, tau-bonds), the antiperiplanar hypothesis, the classic theory of resonance, and the preference for staggered bonds over eclipsed bonds in tetrahedral systems, a simple qualitative model is presented to rationalize the conformation and reactivity for a wide range of compounds containing double bonds and/or carbonyl groups. Alkenes, carbonyl and carboxyl derivatives, conjugated systems as well as other functional groups are revisited. This also leads to a simple model to understand aromaticity, and electrocyclic reactions. The bent bond model and the antiperiplanar hypothesis provide a qualitative model for better understanding the electron delocalization and the reactivity inherent to unsaturated organic systems by an alternative view of the classic resonance theory.

<sup>a</sup>Department of Chemistry, University of New Brunswick, P. O. Box 4400, Fredericton, NB, Canada E3B 5A3. E-mail: ghislain@unb.ca

<sup>b</sup>OmegaChem Inc., 480 rue Perreault, St-Romuald, QC, Canada G6W 7V6

<sup>c</sup>Département de Chimie, Université Laval, Québec, QC, Canada G1V 0A6. E-mail: pierre.deslongchamps@chm.ulaval.ca

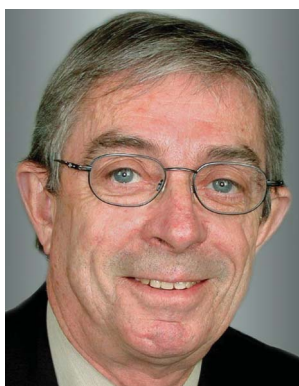
### Introduction

Since the 1930s, two different bonding models have been used to describe the typical unsaturation found in alkenes, alkynes, arenes, as well as various carbonyl-type compounds. Both Slater and Pauling pointed out this ambiguity in how to represent multiple bonds.<sup>1</sup> As shown in Fig. 1, the Hückel model<sup>2</sup> consists of the familiar  $\sigma/\pi$  orbital construct whereas the Pauling model<sup>3</sup> is



**Ghislain Deslongchamps**

Born in Montreal, Quebec, Ghislain Deslongchamps received his B.Sc. at l'Université de Sherbrooke (1984), his Ph.D. at the University of New Brunswick (1989), and was NSERC post-doctorate fellow at MIT under Julius Rebek Jr. (1989–91). After an Assistant Professor appointment at l'Université Laval, he moved to the University of New Brunswick in 1992 where he is currently Professor. He is active in the areas of molecular recognition, medicinal chemistry, asymmetric organocatalysis and computational chemistry. He is also involved in chemical education, having authored "Organic Chemistry Flashware" for online learning. He is currently co-chair of the Gordon Research Conference on Visualization in Science and Education.



**Pierre Deslongchamps**

Born in St-Lin, Quebec, Pierre Deslongchamps received his B.Sc. in Montreal (UdeM, 1959), his Ph.D. in Fredericton (UNB, 1964), and was a postdoctorate fellow at Harvard (1965, R.B. Woodward). He was appointed Assistant Professor at the Université de Montréal and moved to the Université de Sherbrooke in 1967 where he is Emeritus. He was President-Founder of NeoKimia Inc. (1998), now Tranzyme Pharma Inc. He is presently Professeur-Associé at Université Laval and Executive Scientific Advisor at OmegaChem Inc. He has made seminal contributions in the total synthesis of Natural Products and on the concept of Stereoelectronic Effects. He has received many awards including the 1993 Canada Gold Medal in Science. He is FRSC, FRS and was elected Foreign Member of the French Académie des Sciences (Paris).

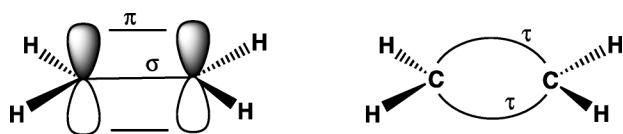


Fig. 1 Hückel model (left) vs. Pauling model (right) of ethylene.

based on two equivalent “bent bonds” (also known as  $\tau$ -bonds, tau-bonds, banana bonds, anti-Hückel bonds). Although the Hückel model has since gained wide adoption,<sup>4</sup> both models are quantitatively equivalent from the standpoint of molecular orbital theory, each being interconvertible *via* unitary transformation of the basic atomic orbital functions.<sup>5</sup> Interestingly, more recent computational work has even suggested that the bent bond model may be preferable in the valence-bond treatment.<sup>6,7</sup>

However, a debate on the validity of one model over the other is not the motivation of this article.<sup>8</sup> Rather, the purpose is to suggest how the consideration of simple concepts, centered on the bent bond valence model, the antiperiplanar hypothesis and classic resonance structures can account for the qualitative interpretation of a remarkably wide range of experimental observations, ranging from conformational analysis, to reactivity and stereoselectivity in various settings. The bent bond model allows for a clear differentiation between the above- and below-plane regions of the structure, and confers ‘stereochemical character’ to unsaturated systems due to the quasi-tetrahedral nature of the bound atoms. Combined with the general concept of Walden inversion when such centers are attacked by nucleophiles, and the advantageous stereoelectronic alignment of various antiperiplanar bonds and lone pairs, this model presents simple visual cues for rationalizing the stereochemical outcome of a wide range of reactions.

## Foundational concepts: $\tau$ hybridization, generalized anomeric effect, and Walden inversion

### $\tau$ Hybridization

The requisite hybridization compatible for forming bent bonds can be rationalized starting from a typical  $sp^2$  hybridized system. Linear combination of one of the  $sp^2$  orbitals with the remaining  $p_z$  orbital produces two orbitals with proper geometries for formation of bent bonds with another atom of similar hybridization. Indeed, re-hybridizing one  $sp^2$  orbital with one  $p$  orbital yields 2 hybrids each with  $1/6$   $s$  character and  $5/6$   $p$  character (Fig. 2).<sup>9</sup> The bent bond model also accounts for the observed bond lengths and angles in a wide range of  $C=C$ ,  $C=X$ , and  $N=O$  compounds.<sup>10</sup>

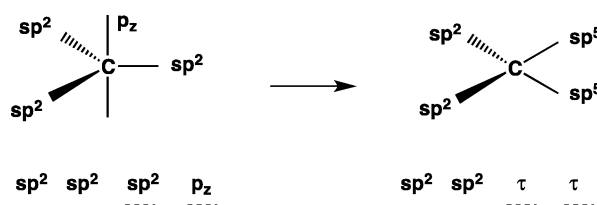


Fig. 2 Hybridization compatible with bent bond formation.

### Generalized anomeric effect

From the original observation of the behaviour of  $\alpha$ - and  $\beta$ -glycosides, the anomeric effect is accepted as a general stereoelectronic phenomenon affecting both conformation and reactivity.<sup>11</sup> Indeed, the presence of a lone pair, antiperiplanar to a polar bond, contributes to the conformational stability and reactivity for a wide range of systems. In acetals and related functional groups, the anomeric effect can be seen from a localized orbital standpoint as a bond/no-bond resonance involving  $n \rightarrow \sigma^*$  interactions, reinforced by the polarity of the adjacent  $C-X$  bond (Fig. 3).

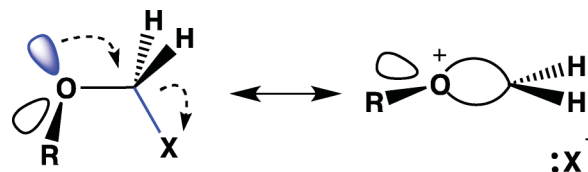


Fig. 3 Bond/no-bond resonance structures describing the anomeric effect as a bent bond.

Thus, glycosidic cleavages can *inter alia* be viewed as the intramolecular  $S_N2$  displacement of a leaving group  $X$  by an antiperiplanar lone pair (aplp); carbonyl and alkene groups can be viewed as two-membered rings. On the other hand, the anomeric effect involving a synperiplanar lone pair is negligible in the ground state based on structural information (X-ray).<sup>12</sup> The result is an elimination assisted ultimately by an aplp.

It is important to note that dashed curved arrows will be used in various resonance structures throughout this article to highlight the stereochemical alignment of structural elements. These are not to be confused with the typical curly reaction arrows (although we do note a growing trend to use curly arrows to interconvert proper resonance structures). Likewise, for representational convenience, some individual resonance structures in the figures may be shown as having slightly different geometries (*i.e.* ground state conformations of isolated Lewis structures). The reader should be mindful that the actual resonance hybrid has a geometry that is intermediate to that of the individual resonance contributors based on their relative energies; the Born–Oppenheimer approximation is valid throughout. Notwithstanding, and as clearly described by Wheland,<sup>13</sup> there can be some, albeit minor, atomic movement between resonance structures if corresponding energetic differences are small. Such is the case of bond/no-bond resonance and of numerous other resonance cases involving anilines, enamines, *etc.* For example, the nitrogen geometry in  $N,N$ -dimethylaniline is intermediate to that of tetrahedral and trigonal centers whereas it is nearly trigonal planar in the 4-dimethylaminopyridine homolog; both of these observations can be accounted by differential contributions from the limiting resonance structures.

### Elimination reactions

The  $E2$  elimination takes place *via* either the *anti* or the *syn* pathway. In the *anti* pathway, the reaction occurs preferentially when the scissile  $H-C$  bond is antiperiplanar to the leaving group (Fig. 4):

In the *anti*-elimination, the reacting molecule is in the lower energy staggered conformation. From the localized orbital

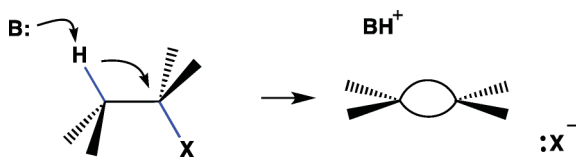


Fig. 4 Anti-elimination, E2 mechanism.

standpoint, the E2 elimination mechanism is viewed as a  $\sigma \rightarrow \sigma^*$  interaction (*i.e.* filled  $\sigma$  orbital of the scissile H–C bond overlapping with the vacant  $\sigma^*$  orbital of the C–X bond). This accounts for the preferred antiperiplanar geometry of the E2 elimination. The corresponding *syn*-elimination is normally less favorable because the reacting molecule is in the higher energy eclipsed conformation. If one assumes antiperiplanarity of all reacting groups, the *syn*-elimination is believed to occur *via* what is known as a “double inversion” pathway according to Ingold and Sicher<sup>14</sup> (Fig. 5). It assumes that, as the base abstracts the hydrogen *cis* to the leaving group X, Walden inversion at the incipient carbanion, facilitated by the relief of eclipsing strain, must take place to allow for antiperiplanar elimination of the leaving group.<sup>15</sup>

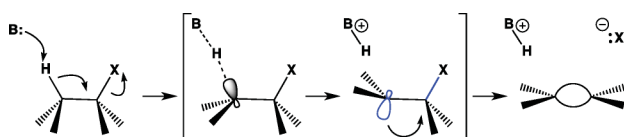


Fig. 5 Syn-elimination, double inversion pathway.

Based on the application of these simple principles, it is now possible to re-examine classical cases of conformational analysis, reactivity, and stereoselectivity, and account for a wide range of experimental observations. Some examples presented herein have been previously described in bent bond formalism but many are accounted with this model here for the first time.

## Conformational analysis in unsaturated acyclic systems<sup>16</sup>

### Alkenes and carbonyl compounds

It is well known that the most stable conformation of propene is actually the staggered structure where one of the methyl hydrogens is *syn* to the vinylic proton (Fig. 6). Note that the staggered/eclipsed labels are reversed compared to those used for the  $\sigma/\pi$  model. As reported by others,<sup>17</sup> the bent bond model accounts for the conformational preference whereby the methyl protons prefer to be staggered with respect to the bent bonds of the alkene ( $\approx 2$  kcal mol<sup>-1</sup> more stable than the eclipsed form).<sup>18</sup> Recall that eclipsed ethane is 3 kcal mol<sup>-1</sup> higher in energy than the staggered form.

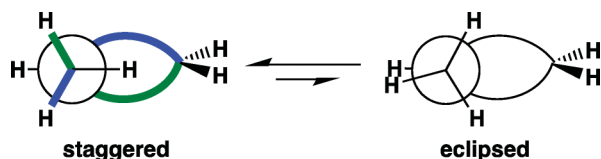


Fig. 6 Conformations of propene.

Preferential staggering of groups adjacent to bent bonds is general. For example, the two lowest energy conformers of 1-butene are both staggered (**1**, Fig. 7).<sup>19</sup> A recent survey of small molecule conformations in both the Cambridge Structural Database (CSD) and the Protein Data Bank (PDB) indicates a preference for the *gauche* form (C=C–C–C dihedral  $\approx 120^\circ$ ) over the *cis* form (dihedral  $\approx 0^\circ$ ) due to lesser allylic 1,3-strain, and virtually no other conformations for 1-butenyl motifs.<sup>20</sup>

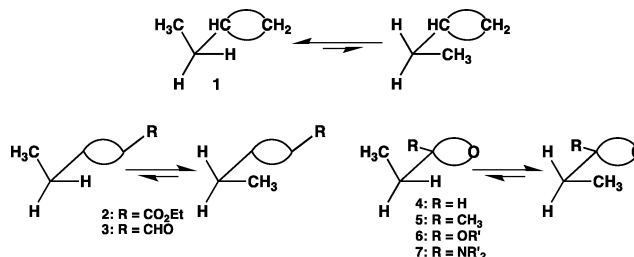


Fig. 7 Most stable conformations of selected unsaturated compounds.

In these staggered conformations, up to two C–H bonds are antiperiplanar to opposing bent bonds that can influence conformation and reactivity *via*  $\sigma \rightarrow \tau^*$  interactions.<sup>21</sup> By analogy to linear  $\sigma$  and  $\sigma^*$  orbitals (**8**), one can view the antibonding  $\tau^*$  orbitals **9** as having a large outer lobe, especially for polarized bonds (Fig. 8). Consequently, lone pairs or bonds antiperiplanar to a given bent bond are in proper alignment for hyperconjugation with the dominant lobe of the neighboring  $\tau^*$  orbital.



Fig. 8 Idealized  $\sigma^*$  C–O (left) and  $\tau^*$  C–O orbitals (right).

Alkene polarization may enhance this hyperconjugative effect to favor *cis* conformers instead. For example, the most stable conformations of ethyl (E)-2-pentenoate **2** and 2-pentenal **3** stagger their terminal methyl between the two alkene bent bonds (Fig. 7).<sup>22</sup> Inomata even coined the term conformational acidity to account for the particular reactivity of these types of conformers in his extensive studies of the related *syn*-effect.<sup>23</sup>

Likewise, acetaldehyde, propionaldehyde **4**, and 2-butanone **5** are most stable in conformations that stagger the adjacent bent bonds, and for the latter two, prefer the conformer where the alkyl group is between the two carbonyl bent bonds (R–C–C=O dihedral  $\approx 0^\circ$ ) by up to 1.2 kcal mol<sup>-1</sup>.<sup>22,24</sup> The same is true for propionate esters<sup>25</sup> **6** and propionamides **7**,<sup>26</sup> but less so for the latter, which have a weaker electron-withdrawing carbonyl that likely induces a lesser anomeric effect with the two antiperiplanar  $\alpha$ -hydrogens. Notwithstanding severe hindrance from large substituents at the  $\alpha$ -carbon, the preferred conformation orients two C–H bonds antiperiplanar to their opposing polar C–O bent bonds.<sup>37</sup>

### Enol ethers/enamines

The preferred conformations of enol ethers, enamines and analogs conform to the bent bond model. Methyl vinyl ether exists

preferentially in the *s-cis* conformation with the *s-trans* about 2 kcal mol<sup>-1</sup> higher in energy.<sup>27</sup> Although dipole arguments have been put forth to account for this contra-steric observation, the *s-cis* conformation staggers the HC–O bond in bent bond formalism where the two oxygen lone pairs are antiperiplanar to two opposing bent bonds (Fig. 9) allowing for anomeric stabilization.

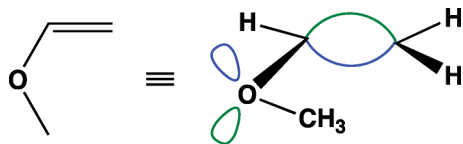


Fig. 9 Preferred *s-cis* conformation for methyl vinyl ether.

The electrostatic rationalization for the *s-cis* conformation is less evident in more conjugated enol ether systems such as compounds **10–12** (Fig. 10), yet they still exist predominantly, if not exclusively, in the *s-cis* form with respect to their proximal alkene group in accord with the bent bond/anomeric model.<sup>28</sup> Even the delocalized iron tricarbonyl complex **12** prefers to orient the alkoxy group *cis* to the region of highest bond order. Sanders referred to the “intriguing possibility” that the Pauling bent bond model could account for their experimental observations.

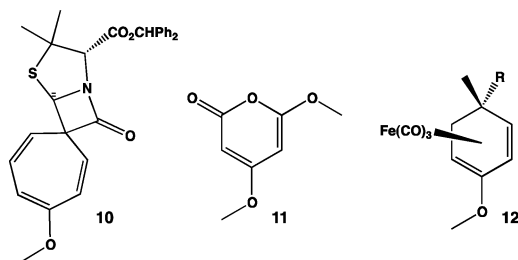


Fig. 10 Preferred conformations for various enol ethers.

Enamines present another interesting case for consideration. In a landmark case, Eschenmoser<sup>29</sup> and collaborators used the bent bond model to account for the observed geometries in a range of crystalline enamines. As shown in Fig. 11, the piperidine enamine **13** has C=C–N–C dihedral angles of ≈0° and ≈136° for the *syn* and *anti* CH<sub>2</sub>–N groups, respectively; the *syn* CH<sub>2</sub> group is staggered between the two bent bonds, and the nitrogen lone pair is antiperiplanar to an opposing bent bond; the nitrogen is thus heavily pyramidalized. For pyrrolidine enamine **14**, the situation is quite different: the angles are ≈7° and ≈176° so both CH<sub>2</sub>–N groups are almost coplanar to the olefin and the nitrogen is essentially planar.

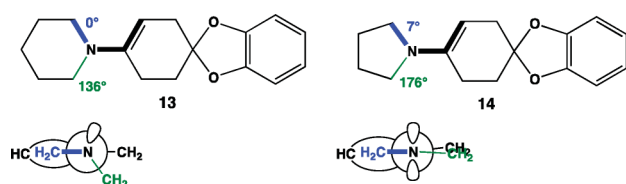


Fig. 11 Dihedral angles in piperidine (**13**) and pyrrolidine enamine (**14**).

Thus, the pyramidal piperidine enamine is best represented by resonance structure **15** that staggers one R–N bond between

the two bent bonds and presents one aplp on nitrogen, *i.e.* an anomeric effect (Fig. 12). On the other hand, due to the 120° angle constraints imposed by the five-membered ring, the planar pyrrolidine enamine is perhaps better represented by considering the alternative charge-separated resonance structure **16** that produces a staggered carbanion and a strong n → τ\* anomeric effect with one of the polar C=N<sup>+</sup> bent bonds. Indeed, X-ray analysis clearly shows that pyrrolidine enamines have a shorter =C–N bond, hence more double bond character, than their piperidine counterparts. This also readily explains the greater nucleophilicity of pyrrolidine enamines *vs.* piperidine enamines toward C-alkylation; it also explains why piperidine enamines are more prone to N-alkylation under the same conditions.<sup>29,30</sup>

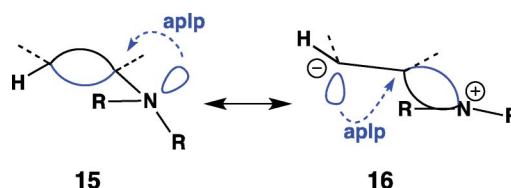


Fig. 12 Bent bond model of enamine resonance structures.

Thus, the characteristic coupling of pyramidalization and rotation of the amino group relative to a planar C=C double bond unit can be readily rationalized in the τ-orbital model, yet again. Of course, the reactivity of these types of enamines can also be rationalized with the σ/π-orbital model and allows direct correlation with photoelectron spectroscopic data.

In another key disclosure by Eschenmoser, a strong case was made for using the bent bond model to account for the stereochemistry of SE'-type reactions, including enamine alkylations.<sup>31</sup> For example, the deuterolytic desilylation of chiral allylsilane **17** gave product **19** almost exclusively, where the departing silyl group and the entering D<sup>+</sup> group are *anti* to each other, in accord with bent bond model **18** (Fig. 13). Likewise, a series of enamines, N,O-acetals (*i.e.* **20** → **21** → **22**), and lactam enolates (*i.e.* **23**) derived from common chiral auxiliaries, all bearing a pyramidal nitrogen with its lone pair antiperiplanar to an opposing bent bond, were shown to undergo C-alkylation preferentially *anti* to the lone pair (*i.e.* **24** → **25**).

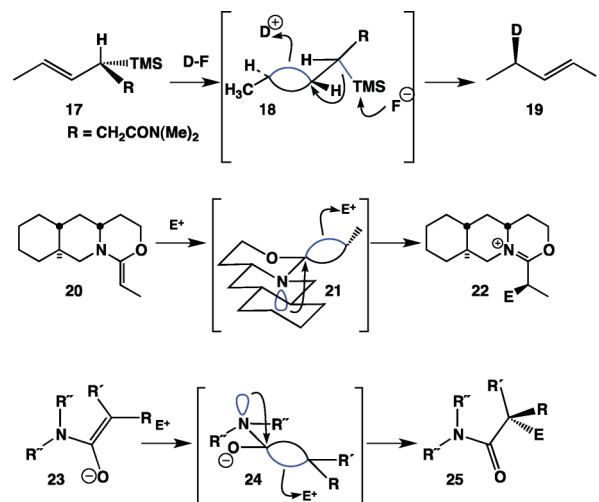


Fig. 13 Preferred *anti* reactivity in a series of SE'-related reactions.

## Esters, lactones and other carboxylic acid derivatives

Esters have been described as having a primary and secondary stereoelectronic effects in the well known  $\sigma$ - $\pi$  bond model (see 26, Fig. 14).<sup>11</sup> Using  $\tau$ -bonds, it is interesting to see that esters, which are known to exist in the most stable *Z*-conformation (even *t*-butyl formate, a serious contra-steric experimental observation),<sup>32</sup> correspond to staggered bent bond model 27 which benefits from two aplp interactions (two  $n \rightarrow \tau^*$ ).

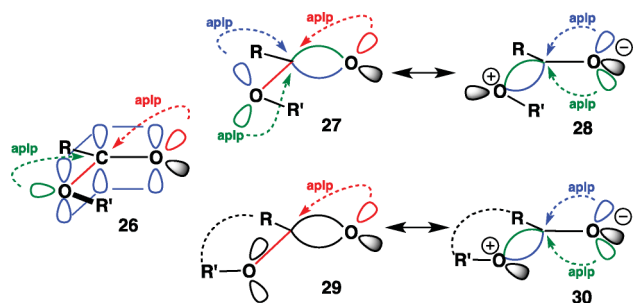


Fig. 14  $\sigma/\pi$  model of *Z*-esters (left) and bent bond models of *E*- and *Z*-esters (right).

In *Z*-esters, it is likely that the alternative charged-separated resonance structure 28 may not contribute much to the hybrid structure as complete electronic delocalization is already achieved in 27. In comparison, the much less stable *E*-ester (*i.e.* lactone) can be described either as resonance structure 29, which eclipses two lone pairs *syn* to the bent bonds (resulting in poor electronic delocalization) or as 30, which gains two antiperiplanar lone pairs (two  $n \rightarrow \tau^*$ ). It is likely that 29 may not contribute as much as 30 even though the latter is a charged-separated resonance structure. This is, however, in agreement with the fact that *E*-esters are generally higher in energy than their *Z*-ester counterparts ( $\approx 3.5$  kcal mol<sup>-1</sup>).<sup>33</sup> The analysis of small-ring lactones (8-membered or smaller) such as  $\delta$ -valerolactone shows that the R-CO-O-R' dihedral angle is near 0°.

Once again, the bent bond model warrants a more detailed consideration of resonance structures, and provides an interesting qualitative tool to account for experimental observations. For example, the carbonyl oxygen of small-ring lactones is more reactive toward electrophiles than that of *Z*-esters. Likewise, the carbonyl carbon of lactones is more reactive toward addition of nucleophiles. Both of these observations are readily accounted by invoking an increased contribution from the charge-separated resonance structure to the overall reactivity in *E*-esters, consistent with their higher energy ground state compared to that of *Z*-esters.

Alkoxy-carbenium ions derived from O-alkylation of  $\delta$ -valerolactones follow suit in similar fashion. X-ray crystallography<sup>34</sup> reveals an in-ring R-COR''-O-R' dihedral angle near 0° and a geometry at the exocyclic OR'' group that is *syn* to the ring oxygen. In bent bond view, the two alkoxy-carbenium resonance structures are no longer equivalent, and stereoelectronic favoring of the endocyclic bent bond may help reinforce the ring planarity found by low-temperature crystallography (Fig. 15). This also explains why the endocyclic R-O bond in alkoxy-carbenium is one of the longest C-O bonds known.

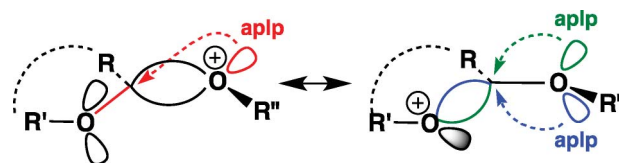


Fig. 15 Resonance structures of alkoxy-carbenium ion in bent bond view.

The bent bond model is also applicable to the observed reaction of lactonium salts with KI where the more hindered ring methylene is displaced preferentially over the methyl group; moreover, a unimolecular reaction occurs preferentially over a bimolecular counterpart.<sup>35</sup> The preferred formation of a *Z*-ester as shown in Fig. 16 is consistent with the iodide attack displacing the more positively charged oxygen.

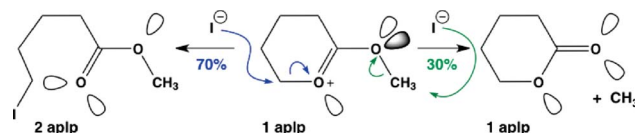


Fig. 16 Reaction of alkoxy-carbenium ion with iodide nucleophile.

The bent bond model accounts also for the greater  $\alpha$ -CH acidity of lactones (*i.e.* *E*-esters) compared to *Z*-esters. Although computational work suggests an important dipolar effect to be operative,<sup>36</sup> a simple analysis of staggered/eclipsed bond interactions can also explain the  $\alpha$ -CH acidity difference.<sup>31</sup> As shown in Fig. 17, *Z*-ester 31 staggers its ether oxygen lone pairs with the carbonyl bent bonds and benefits from two  $n \rightarrow \tau^*$  interactions. Deprotonation of 31 produces enolate 32 where the ether oxygen lone pairs now eclipse the alkene bent bonds with concomitant loss of the  $n \rightarrow \tau^*$  interactions. Lactone 33, in *E*-ester conformation, eclipses its ether oxygen lone pairs with the carbonyl bent bonds and has no  $n \rightarrow \tau^*$  stabilization. Deprotonation of 33 produces enolate 34 where the ether oxygen lone pairs now stagger the alkene bent bonds with concomitant gain of two, albeit weaker,  $n \rightarrow \tau^*$  interactions. This was put forth as a simple explanation for the greater acidity of lactones over *Z*-esters.<sup>31</sup> We wish to add here that lactone 33, regardless of the ring conformation, cannot properly align an  $\alpha$ -CH bond for proton abstraction and delocalization into a carbonyl bent bond to form enolate 34. However, as noted in the preceding section, eclipsing bond interactions present in 33 are completely alleviated in resonance structure 35 where the oxyanion lone pairs now stagger the adjacent bent bond and two strong  $n \rightarrow$

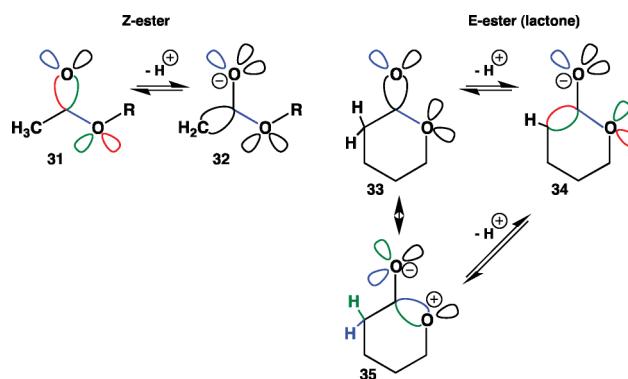


Fig. 17 Bent bond analysis of *Z*- and *E*-ester enolate formation.

$\tau^*$  interactions with the oxenium ion are now evident. The  $\alpha$ -CH bonds in **35** now stagger the oxenium bent bonds, presenting a straightforward stereoelectronic path for forming enolate **34**.

Applying the above analysis of *Z*- and *E*-esters to the unusual C–H acidity of Meldrum's acid ( $pK_a$  DMSO = 7.3) is particularly noteworthy. Meldrum's acid **36** is known to exist in a boat conformation (X-ray) and corresponds essentially to a malonate-like diester where both esters are locked in their *E*-ester conformation (Fig. 18).<sup>31,37</sup> The *E*-ester conformations force the ether oxygen lone pairs to eclipse their adjacent carbonyl bonds (in bent bond view); for such cases, we consider again that the 'minor' ionic resonance structures are important contributors to the overall structure and reactivity as they relieve eclipsed bonds and restore important  $n \rightarrow \tau^*$  stabilizing interactions. Indeed, in structure **36** (**38** in bent bond view) the four ether oxygen lone pairs eclipse the adjacent bent CO bonds so **36/38** has only 2 anomeric effects (*i.e.* one lone pair on each carbonyl oxygen antiperiplanar to an endocyclic C–O bond). Moreover, the two  $\alpha$ -CH bonds in **36/38** eclipse the carbonyl bent bonds and cannot delocalize, regardless of the ring conformation. On the other hand, the ionic resonance structure **37** (**39** in bent bond view) produces four strong  $n \rightarrow \tau^*$  anomeric effects (two per staggered oxyanion) and now positions the  $\alpha$ -CH bonds antiperiplanar to the now staggered bent bonds on the endocyclic oxenium groups. Finally, resonance model **39** accounts well for the remarkable C–H acidity of Meldrum's acid as the abstraction of one of the  $\alpha$ -CH protons in **37/39**, facilitated by two strong anomeric effects, produces enolate **40** stabilized by no less than six anomeric effects! An earlier description of Meldrum's acid using the bent bond model<sup>31</sup> does not consider resonance structure **37/39** as a stereoelectronically relevant contributor to the acidity of Meldrum's acid.

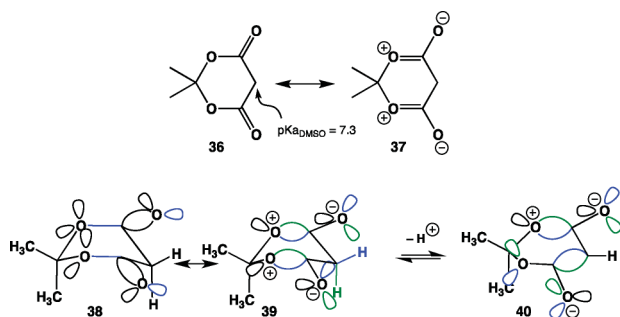


Fig. 18 Meldrum's acid in bent bond view.

The attack of nucleophiles across the electrophilic carbon of alkoxy-carbenium ions derived from  $\delta$ -valerolactone can now be considered. Stereoelectronic principles dictate that nucleophilic addition to a carbonyl group should return a lone pair on oxygen oriented antiperiplanar to the incoming nucleophile (Fig. 19). In what is typically referred to as an "axial attack", addition from one face of a six-membered oxenium ion should produce a chair-like product whereas attack from the opposite face should, at first, produce a twist-boat intermediate that can then transit to a chair form. The attack from the face that directly produces a chair is kinetically favored. This observation can also be rationalized by invoking a quasi in-line  $S_N2$  displacement of one of the two bent bonds in the oxenium ion by the incoming nucleophile in accord with Bürgi-Dunitz.<sup>38</sup>

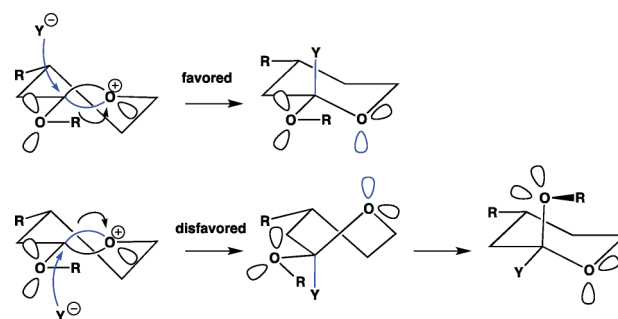


Fig. 19 Reaction of alkoxy-carbenium ion with nucleophiles.

## Amides

The standard  $\sigma/\pi$  model of the amide predicts that the group is essentially planar, and that the nitrogen is  $sp^2$  hybridized (**41**, Fig. 20). The R–C(=O)–N–R' groups of *Z*-amides are essentially coplanar and the barrier for rotating the CO–N bond is  $>20$  kcal mol<sup>-1</sup>. However, the NH proton of 2° amides does not lie completely in the plane and the amide nitrogen is partially pyramidalized. Some experimental and most theoretical structures show some puckering at nitrogen in isolated structures.<sup>39</sup> Many molecular mechanics force fields (*i.e.* MMFF94s) enforce NH planarity in amides, not because of correspondence to a local energy minimum, but for convenience when comparing model proteins to crystal structures in which the exact position of NH protons is time-averaged, influenced by H-bonding, or often undetermined.<sup>40</sup> The bent bond model for amides can account for the quasi-planarity of the R–C(=O)–N–R' component, the greater stability of *Z*-amides over *E*-amides, even the partial non-planarity about the nitrogen. As shown in Fig. 20, the more stable 2° *Z*-amide can be represented as a hybrid of resonance structures **42** and **43**. In **42**, the R' group is staggered between the two  $\tau$ -bonds and the N lone pair is antiperiplanar to an opposing bent bond. The N–H bond is also antiperiplanar to an opposing  $\tau$ -bond, is quite polar, and may still contribute some electronic delocalization (*i.e.* hyperconjugation). The charge-separated resonance structure **43**, which has two  $n \rightarrow \tau^*$  interactions, must also contribute to the hybrid in order to obtain more planarity at the nitrogen atom. The situation is different in the less stable *s-cis* conformer, which is found in *E*-amides and lactams. This conformer cannot be represented adequately by resonance structure **44** alone in which the groups are eclipsed and where there is no anomeric effect (other than the O lone pair antiperiplanar to the C–N bond).

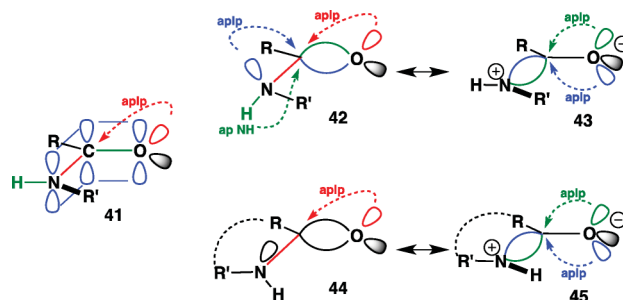


Fig. 20  $\sigma/\pi$  (left) and bent bond models (right) of 2° amides.

On the other hand, resonance form **45**, despite its ionic character, reduces eclipsing interactions and recovers two strong anomeric effects from two lone pairs on the now staggered oxygen with the highly polar C=N<sup>+</sup> bond. Thus, neutral staggered form **42** is better suited to describe the properties of *s-trans* 2° amides while ionic structure **45** may be more representative of the structure and reactivity of its *s-cis* counterpart in their respective hybrid. Of course, a greater ionic character for the *s-cis* form renders it less stable than the *s-trans* form, consistent with experiment.

3° amides can be analyzed in the same fashion by considering resonance structures **46** and **47** (Fig. 21). Structure **46** is staggered but now has only one anomeric effect at nitrogen (no N–H bond) in addition to one aplp at the carbonyl oxygen. In ionic structure **47**, the now staggered oxyanion produces two strong anomeric effects from two lone pairs with the highly polar C–N<sup>+</sup> bonds; two electron-donating alkyl groups at nitrogen also enhance the contribution of resonance structure **47**. All in all, this predicts an essentially planar geometry for sterically unhindered 3° amides, in agreement with X-ray data, and perhaps a greater nucleophilicity at oxygen.

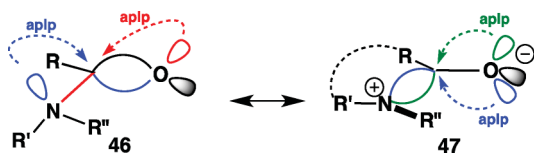


Fig. 21 Bent bond model of 3° amides.

In the final analysis, we remain mindful that amides do not show sufficiently pronounced pyramidalization as to warrant exclusive consideration of the  $\tau$ -bond model to account for their geometric preference.

$S_N2'/E2'$  reactions. The vinylogous  $S_N2$  reaction ( $S_N2'$ ) is known to proceed preferentially by nucleophilic attack *syn* to the allylic leaving group.<sup>41</sup> As noted previously,<sup>37,42</sup> the stereoselectivity of this reaction can be accounted by the bent bond model where the nucleophile displaces the bent bond in  $S_N2$  fashion such that, at the transition state, the incipient carbanion is antiperiplanar to the departing allylic leaving group (**48** → **49**, Fig. 22). Such facial selectivity is not readily evident by the standard orbital model unless  $\sigma/\pi$  orbital mixing is considered.<sup>43</sup>

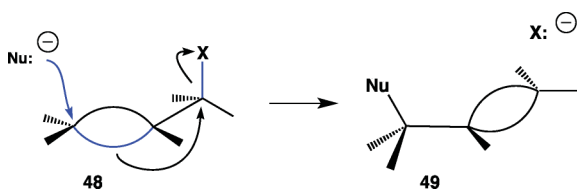


Fig. 22 Bent bond model for the  $S_N2'$  reaction.

In another landmark paper by Eschenmoser, the bent bond model was used to account for the stereoselectivity of  $E'$  and  $E''$  elimination reactions.<sup>42</sup>

For example, decarboxylation of a series of  $\beta,\gamma$ -unsaturated  $\delta$ -hydroxyacids with a mild dehydrating agent (*i.e.*  $E'$  conditions) invariably produced diene isomers in stereoselective fashion (Fig. 23). For example, diastereomer **50** produced *E,E*-diene **51** (96%) whereas diastereomer **52** yielded *E,Z*-diene **53** (93%).

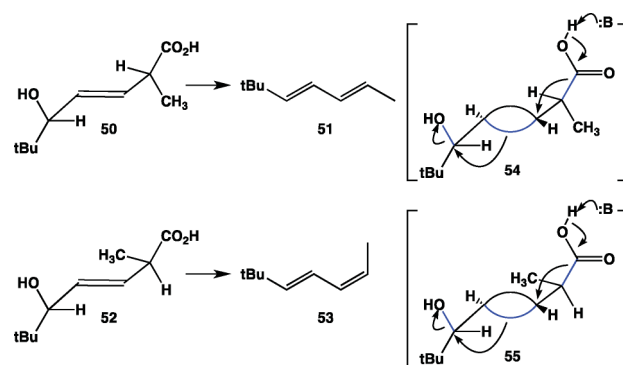


Fig. 23 Stereoselectivity of  $E'$  elimination reactions.

Bent bond models **54** and **55** readily explain the observed stereoselectivities for  $E'$  elimination if one views the decarboxylation as an intramolecular  $S_N2$  displacement of an antiperiplanar bent bond and that the incipient lone pair be antiperiplanar to the hydroxyl leaving group. The **52** → **53** transformation is particularly interesting because of the higher 1,3-allylic strain at transition state **55** leading to *Z*-alkene product **53**.  $E''$  eliminations were shown to be less predictable, presumably due to the highly delocalized nature of the reaction.

### Syn-effect

Inomata's "*syn*-effect" has been recognized as a major cause of stabilizing the *syn* conformation at the transition state of a number of reactions against steric hindrance (Fig. 24).<sup>23</sup> For example, the base-induced isomerization of vinylic sulfones **56** to form allylic sulfones **57** (and various related reactions) under kinetic conditions demonstrate a clear stereochemical preference for products where allylic protons are antiperiplanar to an opposing bent bond at the transition state, leading to *syn* products. In similar fashion, the base-induced desulfonylation of  $\alpha,\alpha$ -dialkylated *E*-allylic sulfones **58** displayed a *syn*-effect as shown by the preferred production of *Z*-dienes **59**. In all cases, the *syn* conformation of these compounds allows for overlap of two allylic C–H  $\sigma$  orbitals with the  $\pi^*$  orbital lobes of the adjacent C=C/C=O bond (*i.e.*  $\sigma \rightarrow \pi^*$  interactions), which has been proposed as a major contributor to the *syn*-effect. Inomata also described the same stereoelectronic effect as  $\sigma \rightarrow \sigma^*$  bent interactions (*i.e.*  $\sigma \rightarrow \tau^*$  interactions) corresponding to bent bond transition state models **60** and **61**. The stereoelectronic preference and related "conformational acidity" of the allylic hydrogens is undoubtedly reinforced by the polarization of the alkene by the attached sulfone.

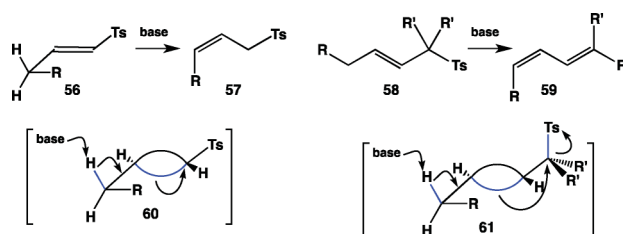


Fig. 24 Bent bond views of the *syn*-effect.

The well-known preferential removal of an  $\alpha$ -hydrogen in ketones and aldehydes to form the corresponding enolate (or enol) is also readily accounted by the  $\tau$ -bond model. As shown by Houk,<sup>44</sup> the preferred conformation for abstracting an  $\alpha$ -hydrogen from acyclic carbonyl compounds is not that where the C–H bond is  $90^\circ$  to the carbonyl, as predicted by the typical “CH- $\pi$  overlap effect”, but rather  $103$ – $105^\circ$  as shown in **62** and **63** (Fig. 25). We note here that this corresponds to dihedral angles of about  $165^\circ$  between the scissile C–H bond and the opposing  $\tau$ -bond of the carbonyl group. This is consistent with Inomata’s kinetic “conformational acidity” concept<sup>23</sup> and with the well known fact that  $\alpha$ -hydrogens that are axially oriented in various cyclohexanone derivatives are preferentially removed under kinetically controlled conditions to form the corresponding enolate.<sup>11,45</sup>

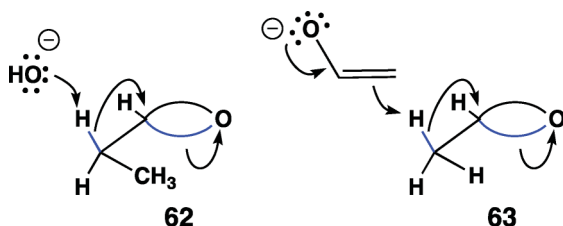


Fig. 25 Base-catalyzed enolization of acyclic carbonyls.

Within the context of enzymatic reactions, one would anticipate reactive conformations of bound substrates to also be compatible with the bent bond formalism. For example, triosephosphate isomerase (TIM), a fundamental component of the glycolysis pathway, interconverts D-glyceraldehyde-3-phosphate (GAP) and dihydroxyacetone phosphate (DHAP) *via* base-catalyzed enolization involving an enediol intermediate (Fig. 26). The side-chain carboxylate of Glu<sub>165</sub> abstracts the pro-R hydrogen at C1 of DHAP and, according to Knowles,<sup>46</sup> the H<sub>pro-R</sub>–C1 bond should be orthogonal to the carbonyl group for proper stereoelectronic alignment (H<sub>pro-R</sub>–C1–C2=O  $\approx 90^\circ$ ) based on the usual  $\pi$ -delocalization model. Crystallographic support for this model originated from a tentative alignment of DHAP into the active site of TIM obtained from enzyme-inhibitor co-crystals (*e.g.* TIM+phosphoglycolohydroxamate, PDB ID: 7TIM) and low-resolution TIM-DHAP structures. However, a more recent high-resolution crystal structure (1.2 Å) of the actual TIM-DHAP complex by Jogl and Tong<sup>47</sup> reveals that the H<sub>pro-R</sub>–C1–C2=O dihedral of the substrate is actually  $160^\circ$ . We note that this angle is much closer to the ideal  $120^\circ$  for  $\tau$ -bond delocalization (*i.e.* **64**) as opposed to the  $90^\circ$  for  $\pi$ -bond delocalization. Interestingly, Jogl and Tong suggested that the H<sub>pro-R</sub>–C1–C2=O dihedral might change from about  $160^\circ$  to  $120^\circ$  just before the reaction.

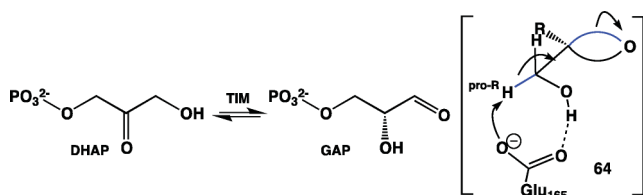


Fig. 26 Catalysis by triosephosphate isomerase.

## Nucleophilic addition on ketones and conjugated ketones

$\tau$ -Bonds, S<sub>N</sub>2-type displacements, and the antiperiplanar hypothesis open an important new and simple understanding of the chemical reactivity of ketones and unsaturated ketones. Hydrides and organometallic nucleophiles add preferentially from the axial face of cyclohexanones (Fig. 27). For example, LiAlH<sub>4</sub> reduction of 4-*t*-butylcyclohexanone gives a 90% yield of the *trans* (*i.e.* equatorial alcohol) product. These observations have been rationalized by what is known as the Cieplak effect,<sup>48</sup> which involves delocalization of axial  $\sigma$  C–H orbitals into the  $\pi^*$  orbital of the carbonyl group. However, we note here that delocalizing electrons into, say, the bottom face of  $\pi^*$ , leads to an even redistribution of electrons on both carbonyl faces due to the symmetry of the  $\pi^*$  orbital. Alternatively, the two axial  $\alpha$ -hydrogens in structure **65** are oriented antiperiplanar to the opposing  $\tau$ -bond of the carbonyl group. Electron donation from those two polar CH bonds into the antibonding  $\tau^*$  orbital of the axial  $\tau$ -bond will clearly render that C–O  $\tau$ -bond more electron-rich than the equatorial  $\tau$ -bond without any symmetry constraints. As a result, a nucleophile will preferentially displace the weaker (*i.e.* electron poorer) equatorial  $\tau$ -bond resulting from an axial attack yielding **66**.

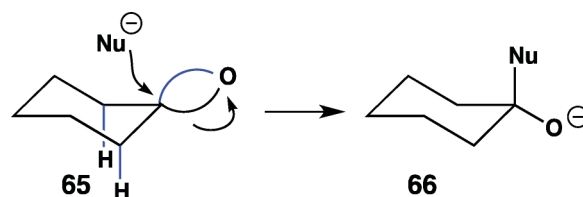


Fig. 27 Nucleophilic addition to cyclohexanone derivatives.

By the same token, various electron-withdrawing (EWG) or electron-donating groups (EDG) present on the cyclohexanone ring will thus influence the relative ratio of axial/equatorial attack by either decreasing or increasing the electron density at one of the two C–O bent bonds based on stereoelectronic alignment (Fig. 28).<sup>49</sup> This is the case for 3-substituted cyclohexanones.

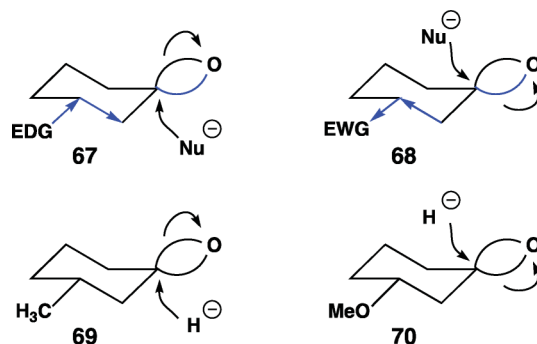


Fig. 28 Substituent effects on nucleophilic addition to cyclohexanone derivatives.

With an EDG (alkyl or TMS) as shown in structure **67**, the C2–C3 bond is electron donating by inductive effect and, because it is antiperiplanar to the equatorial  $\tau$ -bond of the C=O, can enrich the  $\tau$ -bond. Consequently, it is the weaker axial  $\tau$ -bond that



undergoes  $S_N2$ -like displacement by the incoming nucleophile. An EWG ( $CF_3$ ,  $C_6H_4$ ,  $C_6H_5$ , OR,  $CF_3$ ) at C3 will have the opposite effect by depleting the equatorial  $\tau$ -bond as shown in **68**.

This is what is observed experimentally: an EDG disfavors the axial attack whereas an EWG favors it. For example, L-Selectride reduces **69** preferentially from its  $\alpha$ -face whereas replacement of 3- $CH_3$  by 3- $OCH_3$  leads to reduction from the  $\beta$ -face of **70**. In the same vein, epoxidation of cyclohexanones with  $(CH_3)_2SCH_2^-$  occurs preferentially from the axial face.<sup>50</sup> Similar results have been reported for the reduction of 2-alkoxy-4-pyranones.<sup>51</sup>

Despite the high degree of symmetry in adamantanones, rather spectacular stereoselectivity results have been observed.<sup>52</sup> A very simple and clear explanation can be obtained using  $\tau$ -bonds, as an alternative to the Cieplak effect. In the 5-substituted adamantanone **71**, the C-EDG bond is perfectly antiperiplanar to two C-C ring bonds, both of which can donate into the antiperiplanar C-O  $\tau$ -bond on the left (Fig. 29); the weaker  $\tau$ -bond on the right is displaced preferentially by incoming nucleophiles. Likewise, an EWG at the same position (*i.e.* **72**) will render the left  $\tau$ -bond electron poorer so nucleophilic displacement will occur from the right side. This confirms all experiments where an EDG at C5 ( $R = Me_3Sn$ , TMS) directs nucleophilic attack on the left side of the carbonyl group whereas an EWG ( $R = F$ ,  $NMe_3$ ) directs the same reaction on the right side. The preferential facial selectivities for all the reactions shown in **73–78** agree with this analysis. Moreover, when the C=O group of adamantanone is replaced by an exo olefin as in **78**, electrophiles ( $RCO_3H$ ) now react preferentially with the more electron rich  $\tau$ -bond! Thus, the *syn* attack is favoured in **78** when  $R=F$  or  $C_6H_5$  but the *anti* attack is slightly preferred with  $R=TMS$ .<sup>52</sup> Epoxidation (66%) or addition of HCl (99.5%) also takes place from the *syn* side. Interestingly, N-oxide formation of **79** occurs *syn* to the 2° alcohol, *i.e.* the tertiary amine on the left is less basic due to the antiperiplanar relay with the electronegative OH group.

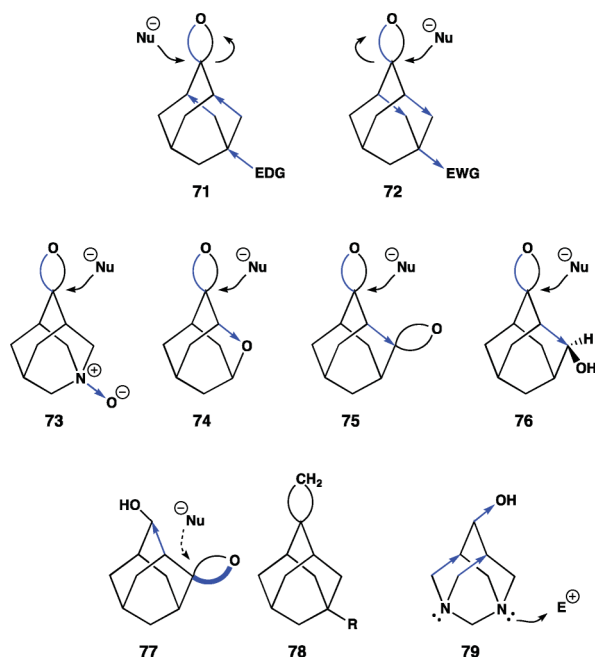


Fig. 29 Preferred stereoselectivity on rigid tricyclic frameworks.

Analogous results have been obtained for norbornenone derivatives **80–82** (Fig. 30).<sup>52</sup> Also, electrophiles react completely *anti* in cyclobutene **83** when  $R=CH_3$ . When the R groups are EWG ( $OSO_2Me$ , Cl, OAc or OMe), the major product obtained is contra-steric, resulting from *syn* addition of the electrophile. The reactivity of all these derivatives is in complete agreement with the simple stereoelectronic and  $\tau$ -bond arguments.

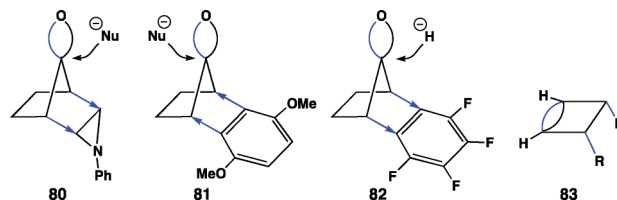


Fig. 30 Nucleophilic addition to norbornenone derivatives.

Another interesting result is the preferred formation of the *syn* product **86** from the nucleophilic addition on the dienone **84** (Fig. 31). Drawn in  $\tau$ -bond model **85**, the two  $\beta$   $\tau$ -bonds at C2–C3/C5–C6, depleted by the antiperiplanar OR' group, are antiperiplanar to the  $\alpha$   $\tau$ -bond of the carbonyl group. The organometallic nucleophile will thus attack *syn* to the R group, displacing the more electron deficient C=O  $\tau$ -bond to yield **86** in agreement with experiment.<sup>53</sup>

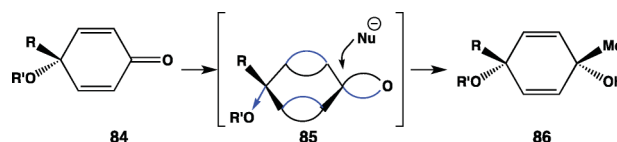


Fig. 31 Nucleophilic addition to cyclohexadienone derivatives.

Ziegler reported highly stereoselective methylenations of alkylidene cyclohexanones *via* 1,2-addition of dimethylsulfonium methylenide (Fig. 32).<sup>54</sup> The observed stereoselectivities for both reactions are consistent with the “axial attack” to cyclohexanones, but can also be accounted by the bent bond formalism.

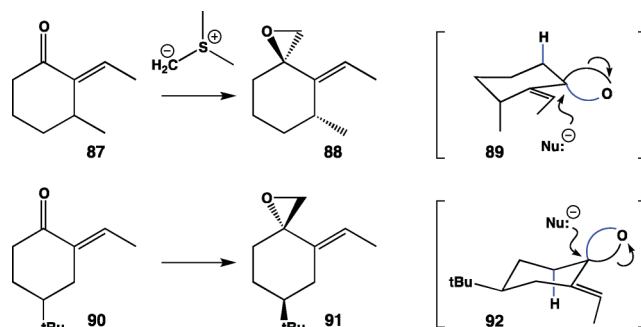


Fig. 32 Nucleophilic addition to alkylidene cyclohexanones.

Indeed, reaction **87**  $\rightarrow$  **88** can be viewed as bent bond model **89** while reaction **90**  $\rightarrow$  **91** can be viewed as bent bond model **92** (note axial hydrogens in both **89** and **92**). What is perhaps more interesting is the fact that in both reactions, due to the conformational skew, the “less conjugated” carbonyl  $\tau$ -bond, that is the one not antiperiplanar to an opposing alkene  $\tau$ -bond, undergoes nucleophilic displacement.

The addition of nucleophiles to acyclic carbonyl groups adjacent to a stereocenter led to several models to explain the experimental results, largely due to uncertainty about the transition state conformations of these compounds. Using a  $\tau$ -bond description, the reactive conformations and direction of nucleophilic attack for the Cram, Karabatsos, and Felkin-Ahn models correspond to Newman projections **93**, **94**, and **95**, respectively, all of which predict the same major product **98** (Fig. 33). Wintner also proposed model **96** based on  $\tau$ -bonds where all the groups are perfectly eclipsed.<sup>37</sup> Interestingly, none of these conformations correspond to staggered conformation **97** (as in propionaldehyde) where the small group S, in occurrence a hydrogen atom, is antiperiplanar to a  $\tau$ -bond. The preferred trajectory for nucleophilic addition at the transition state can be viewed as a displacement of the weaker  $\tau$ -bond that is devoid of anomeric stabilization; this predicts the same product **98**. It would be worth to further test this model theoretically and experimentally.

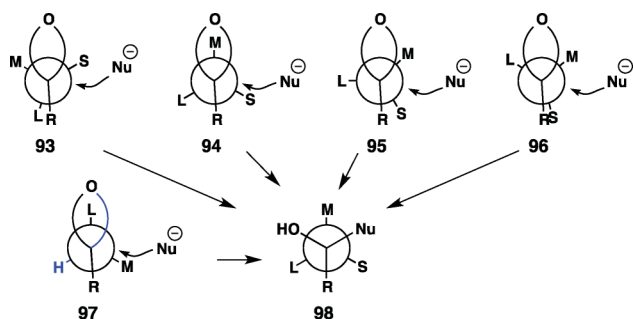


Fig. 33 Nucleophilic addition to  $\alpha$ -chiral aldehydes/ketones.

A most interesting case for consideration is the reaction at the anomeric centre of glycosides, which proceeds through the formation of a cyclic oxenium ion through an  $S_N1$  mechanism or a pseudo-oxenium ion *via* an  $S_N2$  pathway, both proceeding *via* late transition states (Fig. 34).

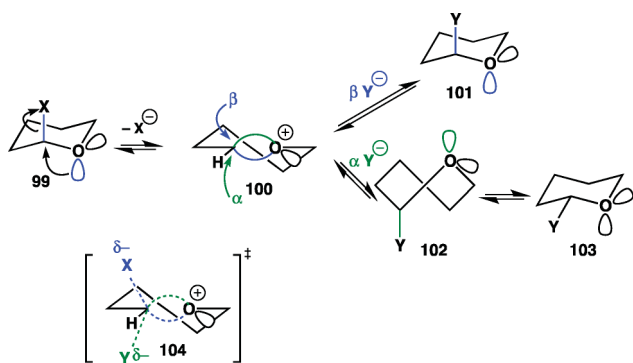


Fig. 34 Substitution at anomeric center.

For the  $S_N1$  pathway, it is easy to see that an  $\alpha$ -glycoside **99** will directly lead to the cyclic oxenium half-chair **100** *via* intramolecular  $S_N2$  displacement. For the reverse process, nucleophilic attack from the  $\beta$ -face with Walden inversion at the anomeric centre will reform product **101** in chair form, whereas similar attack from the  $\alpha$ -face will first produce twist boat conformer **102**, which can then revert to chair **103**. Interestingly, the nucleophilic trajectory follows exactly the Bürgi-Dunitz angle of attack<sup>38</sup> which has

received strong experimental support from X-ray studies. Cyclic iminium ions must also behave in the same manner.<sup>55</sup>

For the  $S_N2$  pathway, bent bond model **104** implies that both the nucleophile Y and the leaving group X will deviate from the  $180^\circ$  ideal to follow the Bürgi-Dunitz trajectory, maintaining antiperiplanarity to the  $\tau$ -bond character of the carbonyl group in the transition state. This could have important implications for a better understanding of the transition states of glycoside hydrolyses (including enzymatic processes), and for the design of glycoside inhibitors; this should be further investigated by theoretical calculation.

The facial selectivity in conjugate additions can also be accounted using the  $\tau$ -bond model (Fig. 35). Axial 1,4-addition of a nucleophile to cyclohexenones **105** can be seen as a relay of antiperiplanar displacements of two bent bonds (*i.e.* **105**  $\rightarrow$  **106**  $\rightarrow$  **107**  $\rightarrow$  **108**). For the equatorial addition, the orbital overlap requirements lead to a higher energy twist-boat-like conformation (**105**  $\rightarrow$  **109**  $\rightarrow$  **110**  $\rightarrow$  **111**).

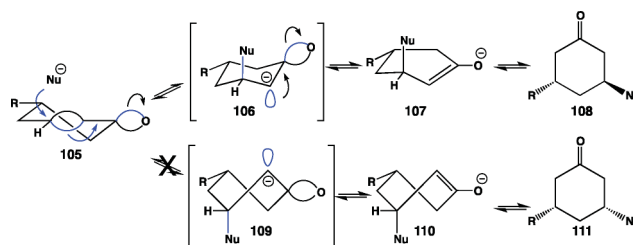


Fig. 35 Conjugate addition to cyclohexenone derivatives.

The presence of EWGs or EDGs at the periphery of enones can also modulate the stereoselectivity of conjugate additions. For example,<sup>56</sup> cuprate addition to 5-substituted cyclopentenone **112** gives mainly the *trans* product **113** (Fig. 36); comparing the stereoselectivity of **112** to that of other 5-substituted cyclopentenones led to the conclusion that this reaction is essentially governed by a novel stereoelectronic effect.<sup>56</sup> Using  $\tau$ -bond description **114**, one can see that the C-OMe bond is antiperiplanar to the  $\alpha$   $\tau$ -bond of the C=O group rendering it electron poor; this  $\tau$ -bond is also antiperiplanar to the  $\beta$   $\tau$ -bond at C2-C3, thus a nucleophile will displace that  $\beta$  C2-C3  $\tau$ -bond yielding the *trans* product **113**.

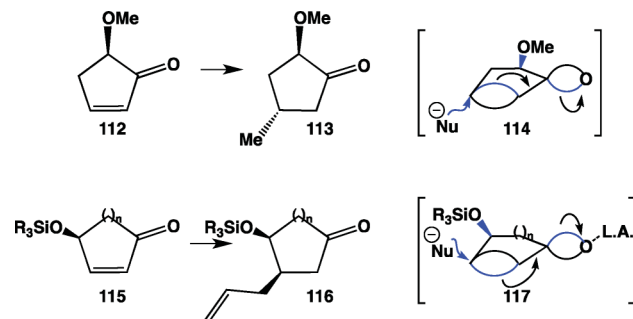


Fig. 36 Conjugate addition to cyclopentenone derivatives.

A similar explanation is readily obtained for the reactivity of  $\gamma$ -substituted enones **115** ( $n = 1$  or  $2$ ), which undergo conjugate addition of allyltrimethylsilane catalyzed by  $TiCl_4$  to give the corresponding *syn* addition products **116**.<sup>57</sup> Yet again, the  $\tau$ -bond description **117** accounts for the observed stereoselectivity. The  $\alpha$

C2–C3  $\tau$ -bond is now weakened by both the antiperiplanar C–OSiR<sub>3</sub> bond and the  $\beta$  C=O  $\tau$ -bond, so conjugate addition of the nucleophile from the  $\beta$  face is favoured giving product **116** despite the contra-steric reaction trajectory.

## Aromaticity and electrocyclic reactions revisited

Considering  $\tau$ -bonds, valence bond theory along with the antiperiplanar hypothesis, we can now revisit aromaticity/antiaromaticity and the well-known thermal electrocyclic reactions.

Cyclobutadiene can be represented as **118** with two  $\tau$ -bonds, which is equivalent to **119** if one highlights the valence electrons of one of the  $\tau$ -bonds (Fig. 37). Note here that, for representational simplicity, the remaining bond between the two top carbons in **119** is shown as a straight line (this simplified visual representation will be used throughout this next section); we do not infer rehybridization between drawings **118** and **119** which, after all, depict the same structure. Note that the singly occupied hybrid atomic orbitals that make up a bent bond are shown as lobes that lie either above or below the molecular plane; thus, in the case of **119** where the upper bent bond is “revealed,” both singly occupied orbitals are above the molecular plane. Let us now allow for a simple extension of the antiperiplanarity tenet used throughout the preceding sections: we allow resonance delocalization to occur only in *anti* fashion such that resonance structure **120** can be generated from **119**. In other words, each electron in **119** can still delocalize but only into the antibonding orbital of a neighbouring  $\tau$ -bond. Note here that the hybrid orbitals in **119** (and other cyclic structures in this section) are no longer perfectly antiperiplanar to their opposing bent bond but are still *anti* to one and *syn* to the other; ideal antiperiplanar relationships are no longer possible in such unsaturated cyclic structures where all the bent bonds eclipse each other, but we retain the term antiperiplanar here to refer to “*anti* across the plane”. We allow only antiperiplanar displacements in generating the various resonance structures.

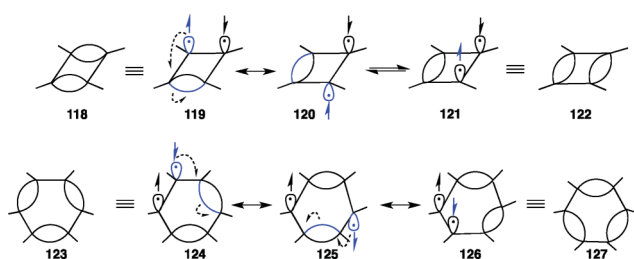


Fig. 37 Cyclobutadiene and benzene.

This extension of the antiperiplanar hypothesis allows the interconversion of resonance structures **119** and **120** without disruption of the singlet state. Note that the hybrid orbitals shown in **120** are *anti* to each other so cannot re-form a  $\tau$ -bond to give the other cyclobutadiene structure **122**. Consequently, the characteristic ring current of aromaticity cannot occur, therefore accounting for cyclobutadiene’s antiaromaticity. The energy barrier for interconverting the two rectangular cyclobutadiene isomers **118** and **122** (short  $\tau$  and long  $\sigma$  bonds) is  $>5$  kcal mol<sup>-1</sup>.<sup>58</sup> According to our model, thermal equilibration can only occur *via*

Walden inversion of one of the radical centers in **120** to produce diradical **121**, which corresponds to the other cyclobutadiene isomer **122**. The energy barrier for Walden inversion is likely higher because anomeric conjugation in **120** must be disrupted during this inversion process; indeed, each radical in **120** is antiperiplanar to a different  $\tau$ -bond.

The situation for benzene, because of its three alternating unsaturations, presents a completely different outcome. In  $\tau$ -bond formalism, benzene can be represented as **123** (or **124** if one wishes to highlight the orbital components of one of the  $\tau$ -bonds). Allowing antiperiplanar displacement of any one of the  $\tau$ -bonds by one of the adjacent orbitals, **124** can be converted to resonance structure **125**. Further antiperiplanar displacement yields resonance structure **126**, which is equivalent to the more familiar representation **127**. One notes immediately that continuation of this antiperiplanar displacement pattern is now compatible with the notion of a ring current consistent with aromaticity. The coplanarity requirement for aromaticity is fulfilled by the requisite antiperiplanar alignments in the ring delocalization. In fact, no atomic motions are implied by the use of representations **123**–**127** to depict benzene. A similar qualitative interpretation of aromaticity/antiaromaticity reported by Rassat<sup>7</sup> invokes heterolytic bond cleavages, although stereochemical character is retained at the carbanions, it is lost at the trigonal carbocation centres. Interestingly, Messmer’s computational work using full generalized-valence bond wave functions concluded that “*Based on energetic considerations, the bent bond model serves as a better framework with which to describe the electronic structure in systems exhibiting resonance than the  $\sigma, \pi$  model.*”<sup>6d</sup>

At this juncture, there is an interesting link here between structure **125** and the bicyclic “Dewar benzene” **128/129** (bicyclo[2.2.0]hexa-2,5-diene, Fig. 38). Homolytic cleavage of the labile central bond in **129** produces diradical **130**, which has a *syn* arrangement of the two radical hybrid orbitals. Resonance structure **131** cannot aromatize unless inversion at one of the radicals were to take place. Note the difference between the formal bond representations of benzene **126** and Dewar benzene **131**. Indeed, inversion at one of the centers in **131** would be required to form benzene; we note that the observed slow conversion of Dewar benzene into benzene is in accordance with our bent bond model, as well as standard orbital symmetry rules.<sup>59</sup>

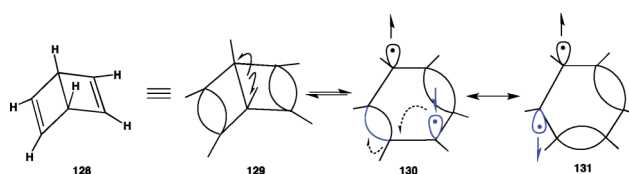


Fig. 38 Dewar benzene.

From the foregoing analysis, one can see that other 4N+2 ring systems will also be aromatic and generate ring current *via* continuous antiperiplanar electronic delocalization of their bent bonds, including aromatic ions. Likewise, 4N ring systems will be antiaromatic.

Electrocyclic reactions can now be considered. Beginning with *cis* 1,3-butadiene **132**, which can be represented as **133**, antiperiplanar delocalization into the adjacent  $\tau$ -bond produces resonance

structure **134** (Fig. 39). Under thermal conditions, only conrotatory ring closure is then possible for **134** yielding cyclobutene **135**, consistent with the Woodward–Hoffmann rules.<sup>60</sup> The process is reversible; indeed, homolytic cleavage of the doubly allylic bond in **135** produces a diradical that, regardless of bond rotation and notwithstanding any radical inversion, must recombine to produce diene **132/133** via antiperiplanar delocalization with the bent bond at C2–C3.

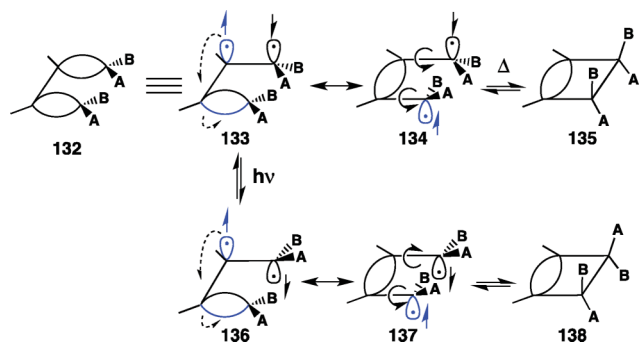


Fig. 39 Cyclization of 1,3-butadiene.

It is important to note here that, for representational simplicity, *cis* 1,3-butadiene **132** (as well as **133/134**) is drawn in the coplanar conformation. This exact geometry is, however, a saddle point; the genuine local minima are *gauche* (i.e. twisted), which produces nice antiperiplanarity between opposing bent bonds.<sup>61</sup>

Photochemically, the cyclobutene–butadiene interconversion is a disrotatory process. Photochemical excitation can be viewed as an inversion at either of the radical centers<sup>62</sup> to produce singlet diradical **136**, followed by antiperiplanar delocalization to produce resonance structure **137**, followed by disrotatory cyclization to yield cyclobutene **138**. The photochemical transition of **133** to **136** can be viewed as a bent bond analog to the  $\pi, \pi^*$  singlet state of ethylene; assuming that one electron from the  $\tau$ -orbital is promoted to the antibonding  $\tau^*$ -orbital, the requisite symmetry inversion can be represented as **136**.<sup>63</sup>

With odd numbers of alternating olefins, such as the case of hexatriene, electrocyclizations will behave in the opposite manner to butadiene. The thermal process will be disrotatory and the photochemical one conrotatory (Fig. 40). Accordingly, structure **139** can be represented as resonance structures **140–142**, which can only yield diene **143** upon thermal disrotatory ring

closure. Likewise, the corresponding photochemical activation will first invert one of the radicals in **140** to produce **144**, which upon antiperiplanar delocalization leads to allowed resonance structures **145** and **146**, and conrotatory cyclization to yield product **147**.

## Conclusions

Combining the  $\tau$ -bond model with the antiperiplanar hypothesis provides a qualitative theoretical basis for better understanding the electron delocalization and the reactivity inherent to unsaturated organic systems by an alternative view of the classic resonance model and modern valence bond theory.<sup>64</sup> The model allows for a clear differentiation between the above-plane and below-plane regions of alkene and carbonyl groups and, because of the tetrahedral nature of the atoms involved, confers “stereochemical character” to these unsaturated systems. On that basis, it allows for a better understanding and predictive tool for analyzing the conformational preference and reactivity for a wide range of functional groups, including alkenes, dienes, enol ethers, enamines, esters, and amides. Stereocontrol in the nucleophilic addition to carbonyls and unsaturated carbonyls, and related reactions is readily understood with a very simple visual model. The concepts of aromaticity/antiaromaticity, and electrocyclic reactions are all accounted by extrapolating the bent bond/antiperiplanar model to cyclic systems. We believe that the  $\tau$ -bond concept first described 80 years ago by Pauling and Slater and invoked by others in sparse disclosures over the years, can still be applied today as a predictive and analytical tool for a surprisingly broad range of organic systems as we have presented here. It should be the subject of more focused experimental and theoretical investigations. Further applications of the bent bond concept to account for pericyclic reactions, including Diels–Alder cycloadditions and sigmatropic rearrangements, will be the subject of subsequent disclosures.

## Acknowledgements

The authors are most grateful to Prof. Jean Lessard (Département de Chimie, Université de Sherbrooke) and to the journal reviewers for their insightful comments and suggestions leading to the final version of this manuscript.

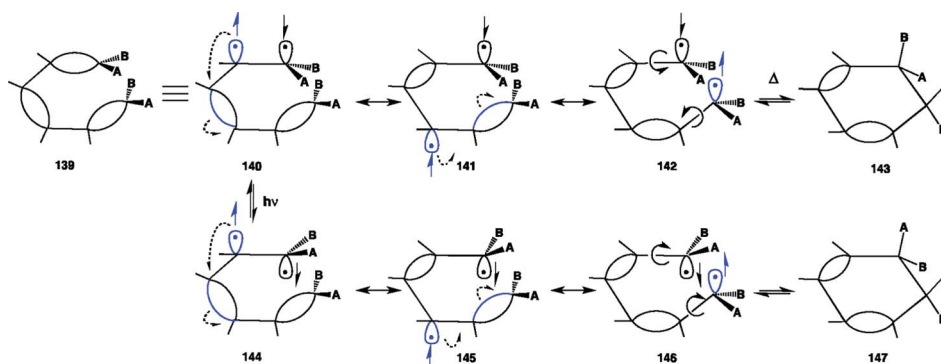


Fig. 40 Cyclization of 1,3,5-hexatriene.

## Notes and references

- (a) J. C. Slater, *Phys. Rev.*, 1931, **37**, 481; (b) L. Pauling, *J. Am. Chem. Soc.*, 1931, **53**, 1367.
- (a) E. Hückel, *Z. Phys.*, 1930, **60**, 423; (b) W. G. Penney, *Proc. R. Soc. London, Ser. A*, 1934, **144**, 166; W. G. Penney, *Proc. R. Soc. London, Ser. A*, 1934, **146**, 223.
- (a) A. Baeyer, *Ber. Dtsch. Chem. Ges.*, 1885, **18**, 2269; (b) L. Pauling, *The Nature of the Chemical Bond*, 3rd ed., 1960, Cornell University Press, pp. 137–138; (c) K. Mislow, *Introduction to Stereochemistry*, W. A. Benjamin: New York, 1966; (d) E. A. Robinson and R. J. Gillespie, *J. Chem. Educ.*, 1980, **57**, 329; (e) J. C. Paniagua, A. Moyano and L. M. Tel, *Int. J. Quantum Chem.*, 1984, **26**, 383; (f) C. E. Wintner, *J. Chem. Educ.*, 1987, **64**, 587; (g) K. B. Wiberg, *Acc. Chem. Res.*, 1996, **29**, 229; (h) F. A. Carroll, *Perspectives on Structure and Mechanism in Organic Chemistry*, Brooks/Cole, Pacific Grove, 1998.
- C. K. Ingold, *Structure and Mechanism in Organic Chemistry*, 2nd Ed., Cornell University Press, Ithaca, 1969, p. 26.
- (a) J. A. Pople, *Q. Rev. Chem. Soc.*, 1957, **11**, 273; (b) K. N. Houk, N. G. Rondan, F. K. Brown, W. L. Jorgensen, J. Madura and D. C. Pellmeyer, *J. Am. Chem. Soc.*, 1983, **105**, 5980.
- (a) W. E. Palke, *J. Am. Chem. Soc.*, 1986, **108**, 6543; (b) P. A. Schultz and R. P. Messmer, *J. Am. Chem. Soc.*, 1993, **115**, 10925; (c) P. A. Schultz and R. P. Messmer, *J. Am. Chem. Soc.*, 1993, **115**, 10938; (d) P. A. Schultz and R. P. Messmer, *J. Am. Chem. Soc.*, 1993, **115**, 10943; (e) F. Ogliaro, D. L. Cooper and P. B. Karadakov, *Int. J. Quantum Chem.*, 1999, **74**, 223–229; (f) V. Gineityte, *Lith. J. Phys.*, 2009, **49**, 389.
- A. Rassat, *Phys. Chem. Chem. Phys.*, 2004, **6**, 232.
- (a) C. W. Bauschlicher Jr. and P. R. Taylor, *Phys. Rev. Lett.*, 1988, **60**, 859; (b) R. P. Messmer and P. A. Schultz, *Phys. Rev. Lett.*, 1988, **60**, 860; (c) G. A. Gallup, *J. Chem. Educ.*, 1988, **65**, 671.
- H. E. Zimmerman, *Quantum Mechanics for Organic Chemists* Academic Press: New York, 1975, pp. 138–140.
- (a) L. Pauling, *The Nature of the Chemical Bond*, 3rd ed., Cornell University Press, NY, 1960, pp. 136–142; (b) E. A. Robinson and R. J. Gillespie, *J. Chem. Educ.*, 1980, **57**, 329.
- (a) P. Deslongchamps, *Stereoelectronic Effects in Organic Chemistry*, Pergamon Press, Oxford, 1983; (b) A. J. Kirby, *The Anomeric Effect and Associated Stereoelectronic Effects at Oxygen*, Springer-Verlag, Berlin, 1983; (c) E. Juaristi and G. Cuevas, *The Anomeric Effect*, CRC Press, Boca Raton, FL, 1995.
- P. Deslongchamps, P. G. Jones, S. Li, A. J. Kirby, S. Kausela and Y. Ma, *J. Chem. Soc., Perkin Trans. 2*, 1997, 2621.
- G. W. Wheland, *Resonance in organic chemistry*, Wiley, NY, 1955, pp. 12–24.
- (a) W. A. Cowdrey, E. D. Hughes and C. K. Ingold, *J. Chem. Soc.*, 1937, 1208; (b) J. Sicher, J. Zavada and J. Krupicka, *Tetrahedron Lett.*, 1966, **7**, 1619.
- (a) J. B. Lambert, *Top. Stereochem.*, 1971, **6**, 19; (b) R. L. Letsinger, *J. Am. Chem. Soc.*, 1950, **72**, 4842; (c) D. Kapeller, R. Barth, K. Mereiter and F. Hammerschmidt, *J. Am. Chem. Soc.*, 2007, **129**, 914.
- E. L. Eliel and S. H. Wilen, *Stereochemistry of Organic Compounds*, Wiley-Interscience, NY, 1994, Chap. 10.
- J. P. Lowe, *Prog. Phys. Org. Chem.*, 1968, **6**, 1.
- D. R. Herschbach and L. C. Krishner, *J. Chem. Phys.*, 1958, **28**, 728.
- (a) D. Van Hemelrijk, L. Van den Enden, H. J. Geise, H. L. Sellers and L. Schäfer, *J. Am. Chem. Soc.*, 1980, **102**, 2189; (b) J. R. Durig, D. A. C. Compton and A. Q. McArver, *J. Chem. Phys.*, 1980, **73**, 719.
- K. A. Brameld, B. Kuhn, D. C. Reuter and M. Stahl, *J. Chem. Inf. Model.*, 2008, **48**, 1.
- P. R. Rablen, R. W. Hoffmann, D. A. Hrovat and W. T. Borden, *J. Chem. Soc., Perkin Trans. 2*, 1999, 1719.
- B. W. Gung and M. M. Yanik, *J. Org. Chem.*, 1996, **61**, 947.
- K. Inomata, *J. Synth. Org. Chem. Jpn.*, 2009, **67**, 1172.
- R. W. Kilb, C. C. Lin and E. B. Wilson Jr., *J. Chem. Phys.*, 1957, **26**, 1695.
- W. B. Schweizer and J. D. Dunitz, *Helv. Chim. Acta*, 1982, **65**, 1547.
- P. Chakrabarti and J. D. Dunitz, *Helv. Chim. Acta*, 1982, **65**, 1555.
- (a) N. L. Owen and H. M. Seip, *Chem. Phys. Lett.*, 1970, **5**, 162; (b) N. L. Owen and N. Sheppard, *Proc. Chem. Soc.*, 1963, 264.
- J. D. Mersh and J. K. M. Sanders, *Tetrahedron Lett.*, 1981, **22**, 4029.
- K. L. Brown, L. Damm, J. D. Dunitz, A. Eschenmoser, R. Hobi and C. Kratky, *Helv. Chim. Acta*, 1978, **61**, 3108.
- (a) A. G. Cook, *Enamines: Synthesis, Structure, and Reactions*, Marcel Dekker New York, London, 1969; (b) S. F. Dyke, *The Chemistry of Enamines*, Cambridge University Press, 1973.
- V. G. Matassa, P. R. Jenkins, A. Kümin, L. Damm, J. Schreiber, D. Felix, E. Zass and A. Eschenmoser, *Isr. J. Chem.*, 1989, **29**, 321.
- M. E. Jung and J. Gervais, *Tetrahedron Lett.*, 1990, **31**, 4685.
- R. Huisgen and H. Ott, *Tetrahedron*, 1959, **6**, 253.
- R. F. Childs, M. D. Kostykc, C. J. L. Lock and M. Mahendran, *Can. J. Chem.*, 1991, **69**, 2024.
- N. Beaulieu and P. Deslongchamps, *Can. J. Chem.*, 1980, **58**, 164.
- K. B. Wiberg and K. E. Laidig, *J. Am. Chem. Soc.*, 1988, **110**, 1872.
- E. M. Arnett, S. G. Maroldo, S. L. Schilling and J. A. Harrelson, *J. Am. Chem. Soc.*, 1984, **106**, 6759.
- H. B. Bürgi, J. D. Dunitz and E. Shefter, *J. Am. Chem. Soc.*, 1973, **95**, 5065.
- J. D. Dunitz and F. K. Winkler, *Acta Crystallogr., Sect. B: Struct. Crystallogr. Cryst. Chem.*, 1975, **31**, 251.
- T. A. Halgren, *J. Comput. Chem.*, 1999, **20**, 720.
- R. M. Magid, *Tetrahedron*, 1980, **36**, 1901.
- E. Vogel, G. Caravatti, P. Franck, P. Aristoff, C. Moody, A.-M. Becker, D. Felix and A. Eschenmoser, *Chem. Lett.*, 1987, 219.
- K. Fukui, *Theory of Orientation and Stereoselection*, Springer-Verlag, 1975.
- S. M. Behnam, S. E. Behnam, K. Ando, N. S. Green and K. N. Houk, *J. Org. Chem.*, 2000, **65**, 8970.
- E. J. Corey and R. A. Snee, *J. Am. Chem. Soc.*, 1956, **78**, 6269.
- J. R. Knowles, *Nature*, 1991, **350**, 121.
- G. Jögl, S. Rozovsky, A. E. McDermott and L. Tong, *Proc. Natl. Acad. Sci. U. S. A.*, 2003, **100**, 50.
- A. S. Cieplak, *J. Am. Chem. Soc.*, 1981, **103**, 4540.
- A. S. Cieplak, B. D. Tait and C. R. Johnson, *J. Am. Chem. Soc.*, 1989, **111**, 8447.
- E. J. Corey and M. Chaykovsky, *J. Am. Chem. Soc.*, 1965, **87**, 1353.
- S. Danishefsky and M. E. Langer, *J. Org. Chem.*, 1985, **50**, 3672.
- M. Kaseji, W. S. Chung and W. J. le Noble, *Chem. Rev.*, 1999, **99**, 1387.
- (a) P. Wipf and Y. Kim, Y., *J. Am. Chem. Soc.*, 1994, **116**, 11678; (b) P. Wipf and J.-K. Jung, *Chem. Rev.*, 1999, **99**, 1469.
- F. E. Ziegler and M. A. Cady, *J. Org. Chem.*, 1981, **46**, 122.
- E. Toromanoff, *Bull. Soc. Chim. Fr.*, 1960, 3357.
- (a) A. B. Smith III, N. K. Dunlap and G. A. Sulikowski, *Tetrahedron Lett.*, 1988, **29**, 439; (b) A. B. Smith III and P. K. Trumper, *Tetrahedron Lett.*, 1988, **29**, 443.
- L. D. Jeroncic, M.-P. Cabal and S. Danishefsky, *J. Org. Chem.*, 1991, **56**, 387.
- G. Maier, R. Wolf and H.-O. Kalinowski, *Angew. Chem., Int. Ed. Engl.*, 1992, **31**, 738.
- E. E. van Tamelen, S. P. Pappas and K. L. Kirk, *J. Am. Chem. Soc.*, 1971, **93**, 6092.
- (a) R. B. Woodward and R. Hoffman, *J. Am. Chem. Soc.*, 1965, **87**, 2511; (b) R. B. Woodward and R. Hoffmann, *The Conservation of Orbital Symmetry*, Academic Press, New York, 1970.
- J. Breuet, T. J. Lee and H. F. Schaefer III, *J. Am. Chem. Soc.*, 1984, **106**, 6250.
- A. Rassat, *Tetrahedron Lett.*, 1975, **16**, 4081.
- R. K. Bansal, *Organic Reaction Mechanisms*, Tata McGraw-Hill, 2001, pp. 456.
- S. Shaik, P. C. Hiberty, *A Chemist's Guide to Valence Bond Theory*, Wiley, NY, 2007.